





STUDY OF CAVITATION EROSION PHENOMENON AT STAINLESS STEEL AISI 304 BASE AND WITH SiC COATING

UDC: 620.193.16

Original scientific paper

<https://doi.org/10.18485/aeletters.2022.7.2.3>

Manuel Vite-Torres^{1*}, Marisa Moreno-Ríos², Arturo Villanueva-Zavala¹, Ezequiel A. Gallardo-Hernández¹, Leonardo Farfán-Cabrera³, Dairo H. Mesa-Grajales⁴

¹Instituto Politécnico Nacional, Grupo de Tribología, ESIME-U.ZAC, Ciudad de México, México

²Tecnológico Nacional de México, Instituto Tecnológico de Pachuca, Pachuca, Hidalgo, México

³Instituto Tecnológico de Monterrey, Campus Puebla, Puebla, Puebla, México

⁴Universidad Tecnológica de Pereira, Colombia

Abstract:

The phenomenon of cavitation erosion consists of the formation, growth, and collapse of bubbles in liquid media. The bubbles are responsible for the damage generated to metal and non-metal materials. Consequently, there is a pronounced degradation on the material surface, producing a scar in the impact area of the bubbles, and eventually the detachment of material. This experimental work aims to determine the performance of AISI 304 stainless steel base and coated with SiC. The SiC coating was obtained by the Chemical Vapor Deposition technique assisted by plasma. The tests were done through an ultrasonic cavitometer with a frequency of 28 kHz in an aqueous medium using tap water. According to the evidence of mass loss, results indicate that the stainless steel coated with SiC have better wear resistance than stainless steel base. In addition, failure mechanisms as cracking, plastic deformation, pits and others, were identified.

ARTICLE HISTORY

Received: 19.10.2021.

Accepted: 02.05.2022.

Available: 30.06.2022.

KEYWORDS

Cavitation erosion, SiC coating, cavitometer, failure mechanisms, wear resistance

1. INTRODUCTION

Cavitation erosion is the mechanical damage of a material caused by the impulsive pressure generated by the continuous collapse of the bubbles [1]. The role of cavitation in machine failure is extremely complex in many aspects [2]. This type of wear occurs for example in propellers [3], hydrofoils [4], pipe bends [5], pumps [6] and hydraulic machinery [7]. The collapse of millions of bubbles can generate fatigue fracture failure or a form of micro fatigue cracking [8-10]. Consequently, detachment of fragments of material occurs. The vibratory and acoustic cavitation equipment leads to formation and collapse of these bubbles.

Furthermore, some experimental studies show that the pressure on the surface caused by the bubbles collapse generate a shock wave range from 1.3 ± 0.3 GPa [11,12]. Patella et al. found the importance of the characteristics and properties of

the materials that are impacted by the bubbles [13]. Hattori et al. [14] performed cavitation erosion tests on S15C carbon steel. They also used high purity aluminium A1070BD-F, which is commonly used in cavitation tests by the vibratory method where the frequency of the oscillator was 19.5 kHz and an amplitude of 50 μm . Moreover, they conclude that the AISI 316L steel presents poor resistance cavitation erosion. Chiu et al. [15] studied the effect of electrolytic hydrogen and its resistance to the phenomenon mentioned above, modifying it with NiTi (Nitinol, nickel-titanium alloy), which they named NiTi-316L coated. The test was carried out according to ASTM G32 standard using deionized water at 23° C. The aim of this study was to describe the effect of electrolytic hydrogen to the resistance of cavitation erosion. Haosheng et al. [16] evaluated the damage caused by cavitation erosion on the surface of 40 Cr industrial steel during the incubation stage, using a cavitometer with a

* CONTACT: M. Vite-Torres, e-mail: drmanuelvite9@hotmail.com

frequency of 20 kHz and an amplitude of 6 μm . Laguna-Camacho et al. [17] carried out another experimental study which objectives were to accelerate the wear damage on the specimens' surface and to simulate more realistic cavitation erosion scenery. Damage was considerably higher and faster when abrasive particles of SiC with a grain size of 75 μm were employed. Bakhshandeh et al. [18] performed tests on a 17-4 precipitation hardening stainless steel substrate coated with electrodeposited Ni/SiC nanocomposite and Ni nanocrystalline, finding that the main failure of the material was due to the synergistic effect of cavitation and corrosion.

The present experimental study determined the damage and degradation suffered by specimens of stainless steel AISI 304 base and coated with SiC under phenomenon cavitation erosion using a cavitometer. In addition, this study led to identification of some main types of failure mechanisms.

2. MATERIALS AND METHODS

2.1 Vibratory cavitation erosion apparatus

The vibratory apparatus or cavitometer was manufactured at Instituto Politecnico Nacional by the Tribology Group of SEPI- ESIME-UZ [19-21]. Fig. 1a and 1b shows a cavitometer based on some parameters of the standard ASTM G32. This equipment converts the electrical energy into kinetic energy using an amplifier that elevates the electrical signal and sends it to a transducer that produces mechanical vibration and transmits it to a horn with a tip made of aluminium 6061.

The tip or vibratory specimen has a circular shape 16 mm in its diameter, and 5 mm of

thickness, its surface was prepared with a 2000 grid abrasive paper and a separation of 12 mm between the surface and the water was found. (see Fig. 1c).

The vibrations are generated at an ultrasonic frequency of 28 kHz \pm 1 kHz, and 50 μm of amplitude, exciting the water and creating bubbles' cloud. The stationary specimen was placed in a specimen holder and was separated separating from the vibratory specimen at approximately 0.5 mm of distance of 0.5 mm, (see Fig. 2).

2.2 Materials

Test specimens are made of 304 AISI stainless steel. Their chemical composition is show in Table 1 [22]. These specimens have a circular shape with 19 mm of diameter and 2.5 mm of thickness, their surfaces were prepared with a 600-grid abrasive paper and cleaned with acetone.

The SiC coating used for this experimental work was 1 μm thick. This coating was produced through the plasma enhanced chemical vapor deposition technique using a continuous discharge with an electrical potential of 900 V inside a reactor manufactured in a Pyrex glass tube of 800 mm and 150 mm internal diameter. On the other hand, the precursor substance used is hexamethyldisilazane (HMDS) - $\text{CH}_3\text{SiH}_2\text{SiH}_2\text{CH}_3$, and the gas mixture was methane (CH_4 UA, ultra-high purity) and UAP argon NH.

In addition, the samples were heated at a temperature of 500° C using an internal resistance located in the sample holder. The deposition time was in a range of 15 to 60 min, and the optimal pressure was 100 Pa. The SiC coating was deposited on 304 AISI stainless steel substrate, (see Fig. 3).

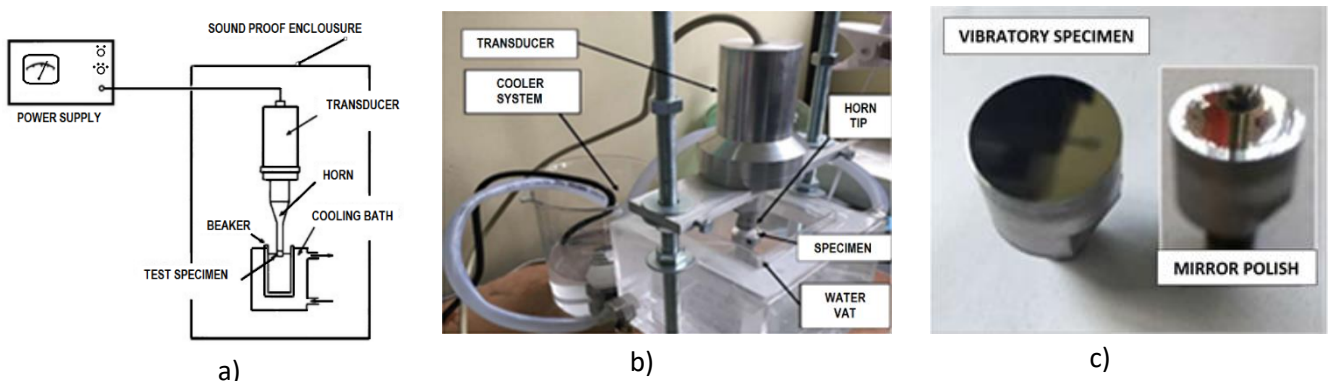


Fig. 1. Vibratory Cavitation Erosion Apparatus, a) schematic diagram, b) manufactured equipment, c) vibratory specimen

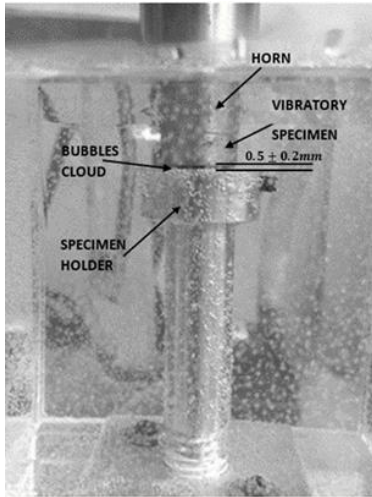


Fig. 2. Forming bubbles in process of cavitation erosion

Table 1. Chemical Composition of 304 AISI Stainless Steel

Element	%
C	0.099 ±0.001
Cr	16 ±1
Ni	8.6 ±0.20
Mn	1.19 ±0.05
Si	0.323 ±0.002
Mo	0.197 ±0.003
W	0.013 ±0.002
Nb	0.0104 ±0.0005
V	0.045 ±0.0003
Ti	+ 0.0080 ± 0.0003
S	0.030 ± .0001

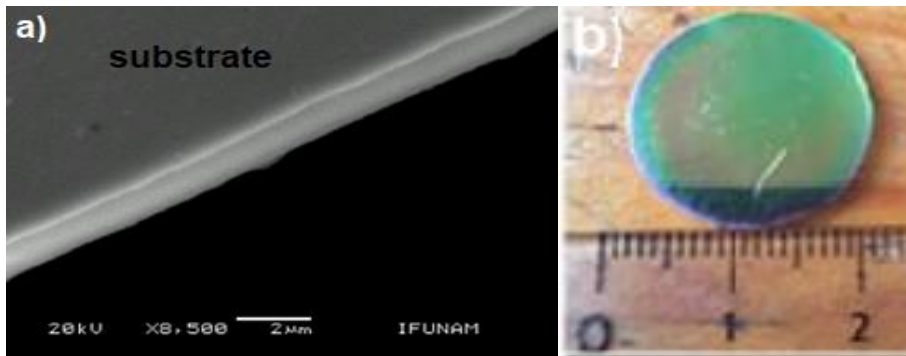


Fig. 3. SiC coating a) SiC cross section SEM, b) SiC coating deposited on stainless steel 304 AISI substrate

2.3 Cavitation erosion test

The surface roughness was measured with a Galaxy Gr 260 rugosimeter. To evaluate the hardness, a Vickers Hardness Tester (HV) with a pyramidal diamond indenter LECO LM 700 was used. The Table 2 display AISI 304 stainless steel and AISI coated SiC mechanical properties.

Table 2. Mechanical properties of materials

Material	AISI 304 stainless steel	AISI 304 stainless steel coated SiC
Roughness (Ra, μm)	0.8	0.151
Vickers Micro-hardness load= 300 gf	190	2700 ±364

The vat was cooled using a recirculation of water with a concentration of 4% of ethylene glycol. Then, the media temperature test ranged from 22 – 28 °C. Total time tests were of 20 h and were removed each hour. First, the vat was cleaned with alcohol and acetone. Secondly, the specimen was cleaned with alcohol and distilled water, and was dried with a hairdryer. Each hour was evaluated weigh using a

BOECO BAS analytical balance with a 0.0001 g precision. An Iroscope MG-64 optical microscopy was employed to analyse the surface damage on the specimen by cavitation erosion. Profiles of the specimen worn surfaces were obtained using a BRUKER Contour-X100 optical profilometer, volumetric wear was calculated using equation (1) and the average thickness of material eroded from a specified surface area was calculated by mean depth of erosion (MDE) [19], (see equation 2):

$$V = \frac{m}{\rho} \quad (1)$$

where m is the mass loss and ρ is the material density

$$MDE = \frac{\Delta w}{\rho A} \quad (2)$$

where Δw es the measured mass loss, ρ is the material density and A is the area of the specified surface.

2.4 Results

Fig. 4, 5, 6, and 7 show the results from the cavitation erosion tests. The progressive

degradation on the specimen surface AISI 304 stainless steel base and SiC coated are displayed in Fig. 4.

The final profiles of the specimen's worn surfaces were obtained after a 20 h test is show in the Fig. 5.

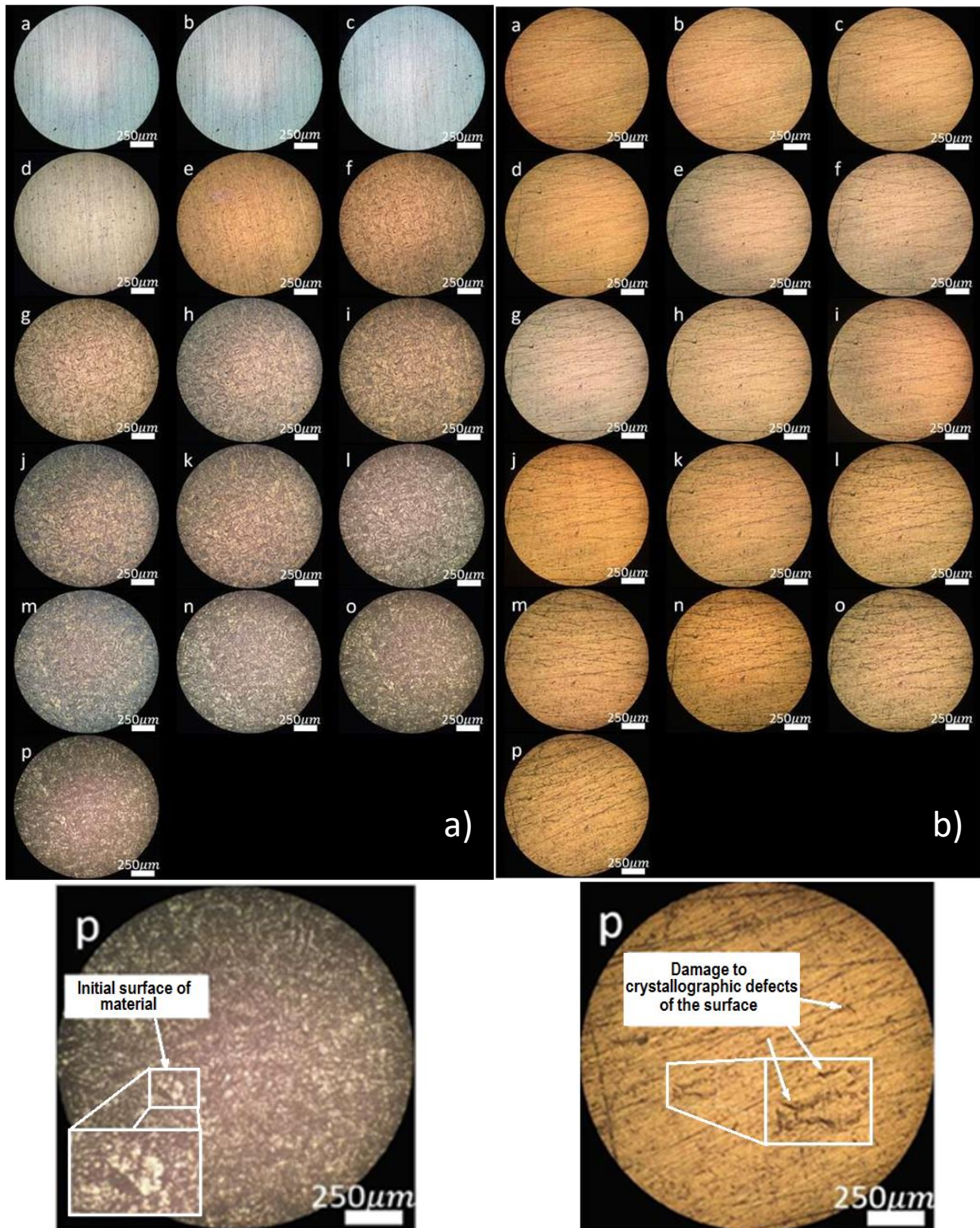


Fig. 4. Progress of surface damage in specimens during the different time intervals.

a) AISI 304 stainless steel base a) 0 h, b) 1 h, c) 2 h, d) 3 h, e) 4 h, f) 5 h, g) 6 h, h) 7 h, i) 8 h, j) 9 h, k) 10 h, l) 12h, m) 14 h, n) 16 h, o) 18 h, p) 20 h, **b)** AISI 304 stainless steel coated SiC a) 0 h, b) 1 h, c) 2 h, d) 3 h, e) 4 h, f) 5 h, g) 6 h, h) 7 h, i) 8 h, j) 9 h, k) 10 h, l) 12 h, m) 14 h, n) 16 h, o) 18 h, p) 20 h

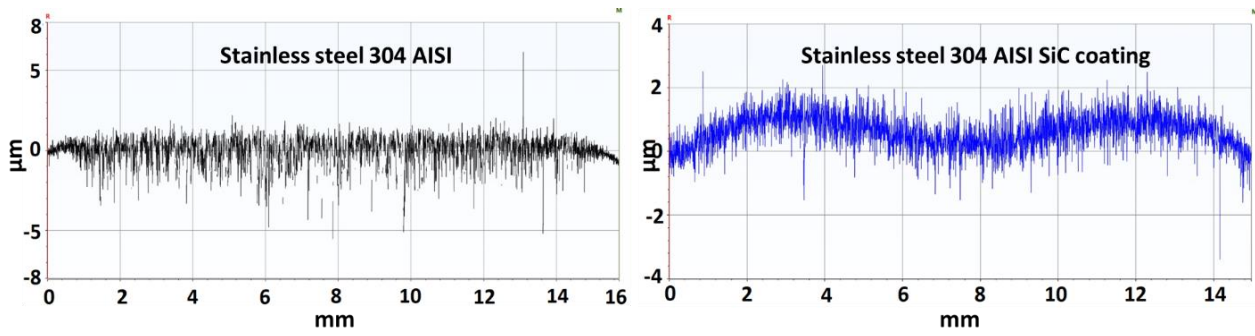


Fig. 5. Profiles of the specimens worn surfaces after 20 h: a) stainless steel 304 AISI base, b) stainless steel 304 AISI SiC coating

For lost volume comparison between AISI 304 Stainless Steel base and AISI 304 Stainless Steel with SiC coating, see Fig. 6.

Whereas the main failure mechanisms identified in stainless steel specimens were pitting, plastic deformation fracture, and scratches, in SiC coated stainless steel were plastic deformation, pitting, and fissure, as displayed in Fig. 7.

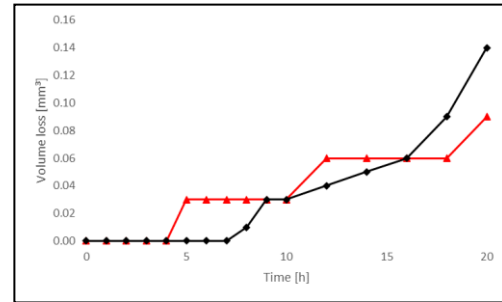


Fig. 6. Volume loss by cavitation erosion a) ■ AISI 304 stainless steel base, b) ▲ SiC coating on AISI 304 stainless steel

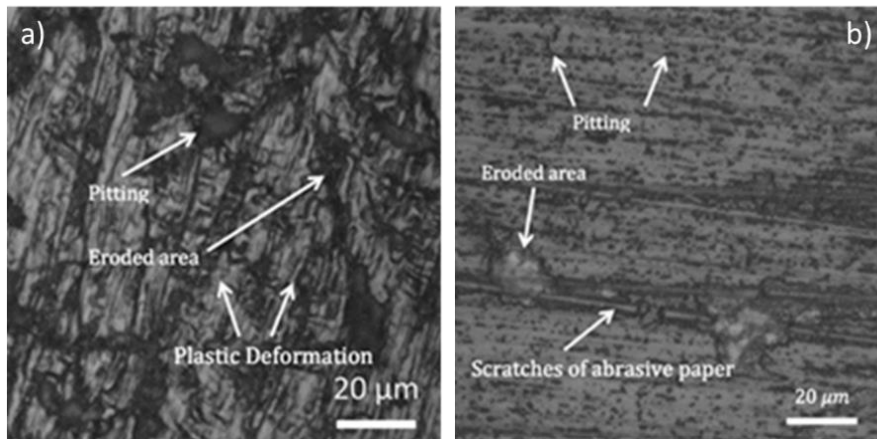


Fig. 7. Mechanisms wear Magnification X50. a) AISI 304 stainless steel base, b) AISI 304 stainless steel with SiC coating

3. DISCUSSION

Fig. 5 shows the damage that appeared on the AISI 304 stainless steel base surface during the first hours of the process, principally in the border of grains due to the austenitic structure that this type of steel has [23].

After 4 h test, the material began to erode without damaging the grains surface. However, the damage was remarkable after 6 h when pitting appeared at some parts of the eroded surface as seen in Fig. 4 g.

Some pitting emerged after 6h of testing, (see Fig. 4 g) with erosion on the stainless steel AISI 304

coated with SiC. Then, after 8h plastic deformation appeared in the grain edge of the SiC.

In addition, the AISI 304 stainless steel is more ductile than the SiC coated, thus the specimen of steel exhibited more plastic deformation than the coating mentioned above. Nevertheless, fatigue in the SiC coating for a long time, induced plastic deformation. Then it broke the weakest areas and exposure to material.

Later, after 9 hours of testing, the plastic deformation was more severe and finally, the material was fractured. The mean depth of erosion was 0.13 μm . Consequently, there was material detachment in the weakest areas as the case of

crystalline structure of stainless steel. Finally, after 10 h of testing, the erosion of the material became progressive, reaching a mean depth of erosion of 0.69 μm .

Regarding SiC coating deposited on the AISI 304 Stainless Steel, after 4 h of testing, deformations appeared without detachment of material. Subsequently, after 6 hours of testing, superficial damages such as pitting appeared on the SiC coating without exposing the stainless-steel substrate. This produced plastic deformation. Finally, after 20 h of testing, a complete detachment of the SiC coating took place, and the mean depth or erosion was 0.47 μm .

The profile of the wear scar of the AISI 304 base stainless-steel specimen showed uniformity. Nevertheless, small alterations caused by the surface undulations of the metallic substrates were observed. These undulations caused deformations in some areas with more exposure to cavitation erosion. This damage in the scar wear reached 5 μm depth ridges periphery of wear scar on SiC-coated stainless-steel specimen, exhibited a profile of 1 μm of depth approximately. This last profile can be explained by the effect of bubbles cloud that were concentrated especially on the edge of the vibratory specimen. For this reason, damage is more severe. In addition, the SiC coating performed very resistantly to cavitation erosion which was in its incubation period where mass losses were practically negligible and only damage appeared due to plastic deformation.

Consequently, it was lesser the lost volume in stainless steel specimen with coating SiC than the lost volume of the 304 AISI stainless steel base specimen as shown in Fig. 6.

The failure mechanisms identified in the 304 AISI stainless steel base were plastic deformation, fractures, scratches, and pitting. In the case of SiC coating, plastic deformation and pitting occurred. Later, fracture occurred, which led to detachment of the material of the coating.

4. CONCLUSIONS

Stainless steel AISI 304 coated with SiC was more resistant than the uncoated stainless steel AISI 304 exposed to cavitation erosion. The SiC coating avoided the plastic deformation in the AISI 304 stainless steel substrate at the beginning of the test. While the test was carried out, scratches, deformations, and pits at the highest borders of the grains appeared due to more concentration of bubbles cloud and more material was lost.

At the end of the test, there appeared severe detachment of the SiC coating appeared, and the material was exposed to the surrounding.

ACKNOWLEDGEMENT

COFAA and SIP to Instituto Politécnico Nacional for the financial support for this work.

NOTE

The abstract of this paper is published at the 10th International Conference on Tribology - BALKANTRIB'20 organised in Belgrade, on May 20-22, 2021.

REFERENCES

- [1] T. Okada, Y. Iwai, Cavitation Erosion, JSME International Journal. *Series I, Solid mechanics, strength of materials*, 33(2), 1990: 128-135. https://doi.org/10.1299/jsmea1988.33.2_128
- [2] F.B. Peterson, Physics associated with cavitation induced material damage, *The 19th meeting of the Mechanical Failures Prevention Group*, 31 October and 1 and 2 November, 2014, at the National Bureau of Standards in Boulder, Colorado, USA, pp.3-12.
- [3] T. van Terwisga, E. van Wijngaarden, J. Bosschers, G. Kuiper, Achievements and challenges in cavitation research on ship propellers. *International Shipbuilding Progress*, 54 (2-3), 2007: 165-187.
- [4] R.E.A. Arndt, Some Remarks on Hydrofoil Cavitation. *Journal of Hydrodynamics*, 24, 2012: 305-314. [https://doi.org/10.1016/S1001-6058\(11\)60249-7](https://doi.org/10.1016/S1001-6058(11)60249-7)
- [5] M. Sathasivam, Dr.J. Tharrini, N. Sarath Kumar, S.J. Sanjeykumaran, Review on cavitation analysis in pipes. *International Journal of Civil Engineering and Technology*, 9 (10), 2018: 1231-1238.
- [6] L. Xian-wu, J. Bin, T. Yoshinobu. A review of cavitation in hydraulic machinery. *Journal of Hydrodynamics*, 28, 2016: 335-358. [https://doi:10.1016/S1001-6058\(16\)60638-8](https://doi:10.1016/S1001-6058(16)60638-8)
- [7] E. Niazi, M.J. Mahjoob, A. Bangian, Experimental and Numerical Study of Cavitation in Centrifugal Pumps, *ASME 10th Biennial Conference on Engineering Systems Design and Analysis 2010, (ESDA 2010)*, 12-14 July, Istanbul, Turkey, pp.1-6.

- [8] A. Vencel, A. Rac, Diesel engine crankshaft journal bearings failures: Case study. *Engineering Failure Analysis*, 44, 2014: 217-228.
<https://doi.org/10.1016/j.engfailanal.2014.05.014>
- [9] R.T. Knapp, J.W. Daily, F.G. Hammitt, Cavitation. *Journal of Fluid Mechanics*, 54 (1), 1970: 189-191.
<https://doi.org/10.1017/S0022112072220614>
- [10] J. Muñoz-Cubillos, J.J. Coronado, S.A. Rodríguez, On the cavitation resistance of deep rolled surfaces of austenitic stainless steels. *Wear*, 428-429, 2019: 24-31.
<https://doi.org/10.1016/j.wear.2019.03.001>
- [11] E.A. Brujan, T. Ikeda, Y. Matsumoto, On the pressure of cavitation bubbles. *Experimental Thermal and Fluid Science*, 32 (5), 2008: 1188-1191.
<https://doi.org/10.1016/j.expthermflusci.2008.01.006>
- [12] M. Paolantonio, S. Hanke. Damage mechanisms in cavitation erosion of nitrogen-containing austenitic steels in 3.5% NaCl solution, *Wear*, 464-465, 2021: 203526.
<https://doi.org/10.1016/j.wear.2020.203526>
- [13] R. Fortes Patella, A. Archer, C. Flagel, Numerical and experimental investigations on cavitation erosion, *26th IAHR Symposium on Hydraulic Machinery and Systems 2012*, 19-23 August, 2012, Beijing, China, pp.022013.
- [14] S. Hattori, T. Ogiso, Y. Minami, I. Yamada, Formation and progression erosion surface for long exposure. *Wear*, 265 (11-12), 2008: 1619-1625.
<https://doi.org/10.1016/j.wear.2008.03.012>
- [15] K.Y. Chiu, F.T. Cheng, H.C. Man, Cavitation erosion resistance of AISI 316L stainless steel laser surface modified with NiTi. *Materials Science and Engineering*, A. 392 (1-2), 2005: 348-358.
<https://doi.org/10.1016/j.msea.2004.09.035>
- [16] C. Haosheng, Li, Jiang, C. Darong, W. Jidao, Damages on steel surface at the incubation stage of vibration cavitation erosion in water. *Wear*, 265, (5-6), 2008: 692-698.
<https://doi.org/10.1016/j.wear.2007.12.011>
- [17] J.R. Laguna-Camacho, R. Lewis, M. Vite-Torres, J.V. Mendez-Mendez, A study of cavitation erosion on engineering materials. *Wear*, 301 (1-2) 2013: 467-476.
<https://doi.org/10.1016/j.wear.2012.11.026>
- [18] H.R. Bakhshandeh, S.R. Allahkaram, A.H. Zabihi, M. Barzegar, Evaluation of synergistic effect and failure characterization for Ni-based nanostructured coatings and 17-4PH SS under cavitation exposure in 3.5 wt % NaCl solution. *Wear*, 466-467, 2021: 203532.
<https://doi.org/10.1016/j.wear.2020.203532>
- [19] ASTM G32 Standard Test Method for Cavitation Erosion Using Vibratory Apparatus, 2016.
- [20] M.S. Tovar Oliva, Estudio del Fenómeno de Erosión por Cavitación en Materiales Metálicos, (Master's Thesis). *Escuela Superior de Ingeniería Mecánica y Eléctrica U. Azcapotzalco, Instituto Politécnico Nacional, Ciudad de México, México, 2012.*
- [21] A. Villanueva Zavala, Estudio Experimental del Fenómeno de Erosión por Cavitación en Bronce, Aluminio y Acero Inoxidable con y sin Recubrimiento de SiC (Master's thesis). *Escuela Superior de Ingeniería Mecánica y Eléctrica U. Zacatenco, Instituto Politécnico Nacional, Ciudad de México, México, 2017.*
- [22] V. Di Graci, M. Torres, E. Saúl Puchi, Dureza en Aceros AISI 304 Laminados en Tibio y en Caliente, *X Congreso Iberoamericano de metalurgia y materiales IBEROMET 2008*, 13-17 October, 2008, Cartagena de Indias, Colombia, pp.237-248.
- [23] G. Bregliozzi, A. Di Schino, S.I.U Ahmed, J.M. Kenny, H. Haefke, Cavitation wear behaviour of austenitic stainless steels with different grain sizes, *Wear*, 258 (1-4), 2005:503-510.
<https://doi.org/10.1016/j.wear.2004.03.024>